Spatial Characteristics of Atrial Fibrillation Using the Surface ECG

U Richter[1], M Stridh[1], A Bollmann[2], D Husser[2], L Sörnmo[1]

[1]Signal Processing Group, Dept of Electrical and Information Technology, Lund University, Sweden
[2]Dept of Electrophysiology, Heart Center, University Leipzig, Germany

Abstract

The present study investigates spatial properties of atrial fibrillation (AF) by analyzing VCG loops synthesized from 12-lead ECGs. The atrial signal is extracted using spatiotemporal QRST cancellation, and spatial properties are characterized through joint analysis of successive fixed-length signal segments. The significance of spatial (loop morphology) parameters is studied in relation to AF frequency, hypothesizing that more organized AF, being expressed by lower frequency, is associated with decreased variability in loop morphology. The results showed that loop orientation can be determined from global analysis (i.e., the entire 60-s segment is used) or the mean of segment-based analysis, both types of analysis leading to similar results. The hypothesis that more organized AF is associated with decreased variability in loop morphology was to some extent confirmed for the parameters planarity and planar geometry; for 1-s segments, the correlation to AF frequency was 0.608 ($p \leq 0.001$) and 0.543 ($p \leq 0.005$).

1. Introduction

Several parameters have been suggested to characterize the degree of AF organization from electrogram analysis [1–5], but only very few parameters for noninvasive, ECG-based characterization of which AF frequency is the most studied. Since this parameter is related to atrial refractoriness, it may be considered to reflect AF organization [9].

The present study investigates spatial AF properties by analyzing VCG loops synthesized from the 12-lead ECG, and studies their relation to AF frequency. It is hypothesized that more organized AF, being expressed by a lower frequency, is associated with decreased variability in loop morphology. Figure 1 offers a schematic illustration of the present approach: the relation between atrial organization (lower corner) and loop morphology (upper right corner) is studied indirectly through AF frequency (upper left corner), as the latter quantity can be estimated from the ECG. The spatial properties are not only expressed in terms of loop orientation (i.e., angles of azimuth and elevation), but also in morphologic terms such as planarity and planar geometry of the loops and related temporal variability.

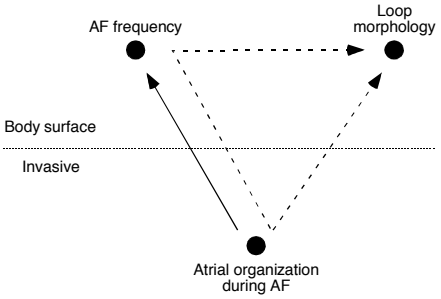

Figure 1. Relation between atrial organization and loop morphology, studied indirectly through AF frequency.

2. Methods

2.1. Preprocessing

The orthogonal leads X, Y, and Z are synthesized from the 12-lead ECG using the inverse Dower transformation [10]. Afterwards atrial activity is extracted through spatiotemporal QRST cancellation [6]. The atrial signal is then decimated from 1000 to 50 Hz since the information of interest is confined to frequencies below 25 Hz.

The spatial properties are characterized by parameters calculated from the entire recording, resulting in "global" values. Spatial variability parameters are calculated from successive fixed-length 1-s segments and expressed in terms of mean and standard deviation. In analogy with [7], segments with lengths related to the dominant atrial cycle length (DACL) are also analyzed. The DACL is here defined as the inverse of the AF frequency, and obtained from the location of the dominant peak in the power spectrum of lead V1. Because the DACL, at times, contains barely one f-wave, the segment length was set to $1.25 \cdot \text{DACL}$.

2.2. Spatial analysis

Orientation

The plane of best fit is defined as the two-dimensional projection of the loop that produces the minimum mean-square error with respect to the original loop. This plane is determined from eigenanalysis of the covariance matrix that results from the $3 \times N$ data matrix with the N samples of the three synthesized leads. This analysis results in the three eigenvectors $\mathbf{v_1}$, $\mathbf{v_2}$, and $\mathbf{v_3}$ associated with the eigenvalues $\lambda_1 \geq \lambda_2 \geq \lambda_3$. The eigenvector $\mathbf{v_1}$ defines the principal axis, i.e., the axis with the largest correlation among the data. The second eigenvector $\mathbf{v_2}$ spans the plane of best fit together with the principal axis. The third eigenvector $\mathbf{v_3} = [\mathbf{v_{3x}}, \mathbf{v_{3y}}, \mathbf{v_{3z}}]^\mathbf{T}$ is the perpendicular axis and defines the azimuth and elevation angles of the plane of best fit (see Fig. 2):

$$\phi_{AZ} = \arctan\left(\frac{v_{3z}}{v_{3x}}\right), \quad (1)$$

$$\phi_{EL} = \left|\arctan\left(\frac{v_{3y}}{\sqrt{v_{3x}^2 + v_{3z}^2}}\right)\right|, \quad (2)$$

where $-90° < \phi_{AZ} < 90°$ and $0 < \phi_{EL} < 90°$. It should be noted that $-30° < \phi_{AZ} < 30°$ corresponds to the sagittal plane, and that $60° < |\phi_{AZ}| < 90°$ corresponds to the frontal plane.

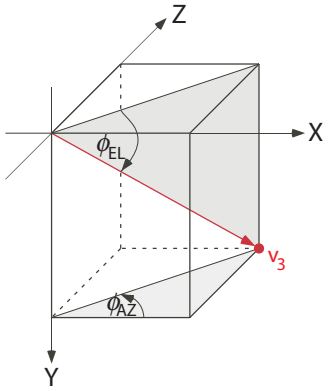

Figure 2. Definition of azimuth ϕ_{AZ} and elevation ϕ_{EL}.

Planarity and planar geometry

Planarity is defined as

$$\psi_{PL} = 1 - \frac{\lambda_3}{\lambda_1 + \lambda_2 + \lambda_3}, \quad (3)$$

and is close to 1 when the loop is essentially planar. Planar geometry is defined as

$$\psi_{PG} = \frac{\lambda_2}{\lambda_1} \qquad \lambda_1 \geq \lambda_2, \quad (4)$$

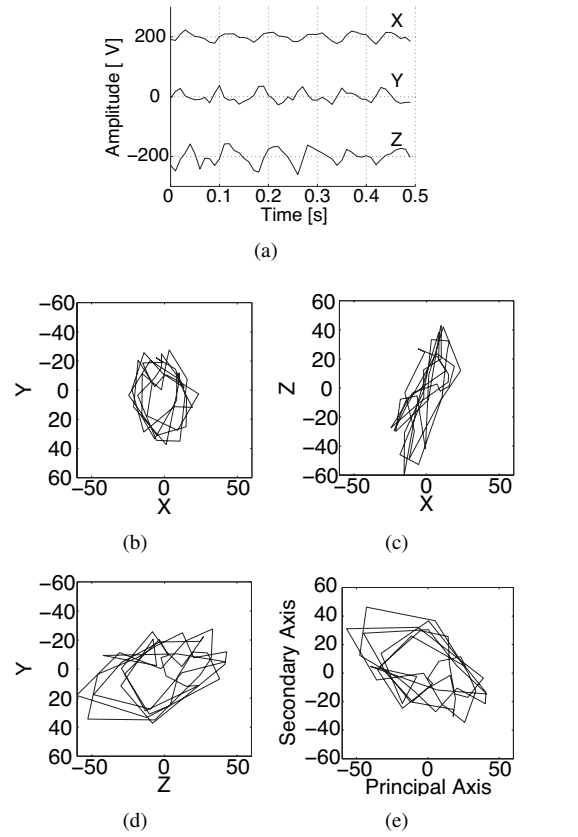

Figure 3. Example of a 1-s segment, containing approximately six f-waves. (a) The orthogonal leads X, Y, and Z after QRST cancellation. (b) Frontal plane. (c) Transverse plane. (d) Sagittal plane. (e) Plane of best fit.

and is close to 1 when the loop is essentially circular.

Figure 3 illustrates the data contained in a 1-s segment. The loops are mostly in the frontal and left sagittal plane, whereas little in the transverse plane; and, consequently, the azimuth angle of the plane of best fit is in the range of the sagittal plane ($\phi_{AZ} = -23.3°$). The elevation angle ϕ_{EL} is $16.7°$. The loops are quite planar ($\psi_{PL} = 0.95$), and have elliptic appearance ($\psi_{PG} = 0.35$).

2.3. Statistical analysis

The correlation between the means as well as the standard deviations (SD) and the AF frequency are calculated, resulting in the correlation value r (Pearson correlation coefficient) and related p-value. A p-value < 0.05 was considered statistically significant.

2.4. Database

The database contains 26 12-lead ECG recordings from patients with chronic AF. All recordings were acquired

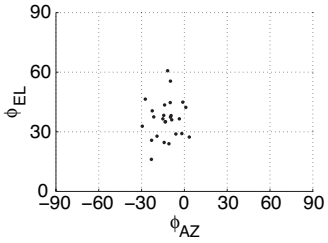

Figure 4. Plot over global azimuth and elevation of each 60 s recording of the database.

with equipment by Siemens-Elema AB, Sweden, using a sampling frequency of 1 kHz and an amplitude resolution of 0.6 μV. The ECGs were recorded during 5 minutes of which 60 s free of ectopic beats were selected for analysis.

3. Results

The AF frequency was estimated with the above described method for each 60-s recording. For the database, the AF frequencies ranged from 3.9 to 7.7 Hz with a mean of 6.4±1.0 Hz (mean $\pm$ SD).

Figure 4 displays global azimuth and elevation of the 26 patients, showing that the azimuth angles are concentrated to the sagittal view. Neither global azimuth ϕ_{AZ} nor global elevation ϕ_{EL} are correlated with AF frequency, as both yielded non-significant p-values. The nature of the data is relatively planar since the global planarity ψ_{PL} is between 0.79 and 0.97. The correlation of ψ_{PL} to the AF frequency is $r = -0.47$ ($p < 0.05$) which indicates a weak trend of ψ_{PL} to decrease with AF frequency. The global planar geometry ψ_{PG} ranges between 0.22 and 0.88. Its positive correlation value of $r = 0.52$ ($p < 0.05$) to AF frequency suggests that the data becomes slightly more circular as AF frequency increases.

The mean azimuth and elevation angles obtained in 1-s segments differ from the global values with only 1.4° and 0.8°, respectively, and planarity and planar geometry with 0.02 and 0.14, respectively. Thus, the results are similar to those of the global parameters, i.e., no correlation between AF frequency and azimuth or elevation, whereas AF frequency exhibits negative correlation with ψ_{PL} ($r = -0.51$, $p < 0.005$) and positive with ψ_{PG} ($r = 0.52, p < 0.05$). The standard deviations of ϕ_{AZ}, ϕ_{EL}, ψ_{PL}, and ψ_{PG} are displayed versus AF frequency in Fig. 5. The standard deviation exhibits a weak trend to increase with AF frequency for ψ_{PL} ($r = 0.61, p < 0.005$) and ψ_{PG} ($r = 0.54, p < 0.005$), suggesting increased variability in waveform morphology. The variability in orientation of the data did not change significantly with AF frequency.

The mean azimuth and elevation angles obtained in DACL-related segments differ from the global values with

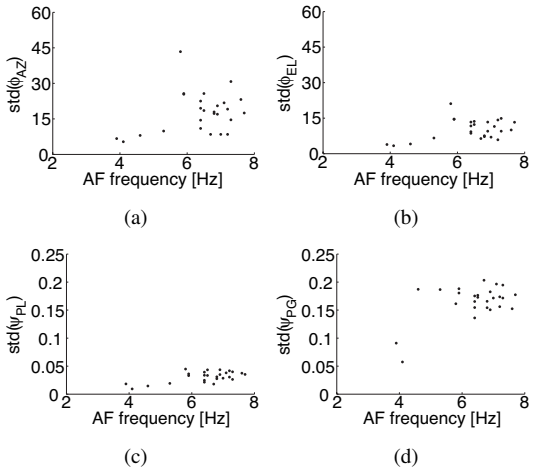

Figure 5. Standard deviation of (a) azimuth, (b) elevation, (c) planarity, and (d) planar geometry as a function of AF frequency. The fixed-length segment was 1 s.

3.4° and 4.3°, respectively, and planarity and planar geometry differ with 0.06 and 0.31, respectively. None of the four parameters are significantly correlated with AF frequency; this result stands in contrast to the results for global and the 1-s parameters, where ψ_{PL} decreases and ψ_{PG} increases slightly with AF frequency. For the standard deviation, there is a tendency to increase with AF frequency, as all correlations exceed 0.5. This result differs from the ones based on 1-s segments, where no correlation was found for the standard deviation of azimuth and elevation.

4. Discussion and conclusions

The calculation of the plane of best fit was previously performed on pure atrial flutter and atrial fibrillation signals, recorded under special conditions [7, 8]. The present paper advances this aspect by combining our spatiotemporal method for QRST cancellation with the calculation of the plane of best fit, offering the possibility to use the method on clinical ECGs.

The distributions of global azimuth and elevation were very concentrated: the angles were located exclusively in the sagittal view. For both evaluated segment lengths, the difference between mean azimuth and elevation and their respective global values was negligible, i.e., the calculation of the angles over 60 s is sufficient as it represents the overall spatial orientation of the data. The analysis of the correlation between AF frequency and global and mean angles, aiming to reveal trends of the parameters for lower and higher AF frequencies, showed that there is no significant difference in orientation between the recordings. This result seems reasonable, as organized and unorganized AF are not known to persist on clearly distinguishable loca-

tions within the atria.

The 1-s variability analysis for azimuth and elevation showed that the standard deviation of the angles over time was relatively low. The standard deviation for the DACL-based segment length was nearly twice as large. This observation can, of course, be a consequence of the shorter segment length, which makes the analysis more sensitive to the actual length of the f-waves as well as to the presence of noise. A reliable trend of the standard deviation with respect to AF frequency could only be identified for the DACL-based segment analysis, i.e., the standard deviation increases with AF frequency. This seems to be reasonable in view of that higher AF frequencies represent less organized AF signals.

We have introduced the parameters planarity and planar geometry for characterization of AF loops. To our knowledge, it is the first time such parameters are applied to atrial activity. The global parameters show that the loops are generally two-dimensional, i.e., planarity is close to one for all recordings. For 1-s segments, the difference between global and mean planarity is negligible, whereas this is not the case for DACL-based segments. Hence, this results in different correlation values: AF frequency exhibits a negative correlation for global planarity as well as mean planarity when calculating with 1-s segments. However, for DACL-based segments, this correlation is not observed. This can be explained by that the spatial extent of about one f-wave is generally very two-dimensional, i.e., the planarity is close to one. Consequently, this yields a high mean planarity, independent of AF frequency. When in contrast the calculation is based on longer sequences, which thus contain several f-waves, two situations arise: When AF is organized and with similar f-waves, which is often the case for low AF frequencies, the loops are situated very close to one plane. When AF is unorganized and with dissimilar f-waves, and often higher AF frequencies, loop planarity decreases, indicating that the f-waves are not close to one plane.

The global values of planar geometry are very scattered, although exhibiting a positive correlation with AF frequency. Similar to planarity, the difference between global and mean planar geometry is negligible for 1-s segments, but not for DACL-based segments. Correspondingly, positive correlation remains for the mean values of planar geometry when calculated for 1-s segments, but disappears for the mean values when the calculation is done for DACL-based segments. This is a result of that the data has elliptic character when segments with one f-wave are used for analysis. When the analysis includes several f-waves, the data will maintain its elliptic character at low AF frequencies, whereas the data becomes more circular, i.e., planar geometry increases, at higher AF frequencies which mostly represent unorganized AF.

The standard deviations of both planarity and planar geometry showed a clearly positive correlation with AF frequency for both evaluated segment lengths, which is reasonable as it implies that the morphology of the data is more stable for lower AF frequencies.

Acknowledgements

D. Husser and M. Stridh are supported by the Volkswagen-Foundation. This study has been performed in part within the NordForsk network “Electrocardiology in Atrial Fibrillation”.

References

[1] Sih HJ, Zipes DP, Berbari EJ, Olgin JE. A high-temporal resolution algorithm for quantifying organization during atrial fibrillation. IEEE Trans Biomed Eng. 1999;46(4):440–450.

[2] Holm M, Johansson R, Olsson SB, Brandt J, Lührs C. A new method for analysis of atrial activation during chronic atrial fibrillation in man. IEEE Trans Biomed Eng. 1996;43(2):198–210.

[3] Lazar S, Dixit S, Callans DJ, Lin D, Marchlinski FE, Gerstenfeld EP. Effect of pulmonary vein isolation on the left-to-right atrial dominant frequency gradient in human atrial fibrillation. Heart Rhythm. 2006;3:889–895.

[4] Haissaguerre M, Hocini M, Sanders P, Takahashi Y, Rotter M, Sacher F, et al. Localized sources maintaining atrial fibrillation organized by prior ablation. Circulation. 2006;112:616–625.

[5] Sanders P, Berenfeld O, Hocini M, Jais P, Vaidyanathan R, Hsu LF, et al. Spectral analysis identifies sites of high-frequency activity maintaining atrial fibrillation in humans. Circulation. 2005;112:789–797.

[6] Stridh M, Sörnmo L. Spatiotemporal QRST cancellation techniques for analysis of atrial fibrillation. IEEE Trans Biomed Eng. 2001;48:105–111.

[7] Ng J, Sahakian AV, Fisher WG, Swiryn S. Surface ECG vector characteristics of organized and disorganized atrial activity during atrial fibrillation. J Electrocardiol. 2004;37:91–97.

[8] Ng J, Sahakian AV, Fisher WG, Swiryn S. Atrial flutter vector loops derived from the surface ECG: does the plane of the loop correspond anatomically to the macroreentrant circuit? J Electrocardiol. 2003;36:181–186.

[9] Bollmann A, Lombardi F. Electrocardiology in atrial fibrillation. IEEE Eng Med Biol Magazine. 2006;25(6):15–23.

[10] Macfarlane PW, Edenbrandt L, Pahlm O. 12-Lead Vectorcardiography. Butterworth-Heinemann; 1995.

Address for correspondence:

Ulrike Richter
Dept. of Electrical and Information Technology, Lund University
Box 118, SE-221 00 Lund
urr@eit.lth.se